ACS APPLIED MATERIALS & INTERFACES

www.acsami.org

Research Article

3D Bioprinting-Tunable Small-Diameter Blood Vessels with Biomimetic Biphasic Cell Layers

Xuan Zhou, Margaret Nowicki, Hao Sun, Sung Yun Hann, Haitao Cui, Timothy Esworthy, James D. Lee, Michael Plesniak, and Lijie Grace Zhang*

Cite This: *ACS Appl. Mater. Interfaces* 2020, 12, 45904−45915

Read Online

ACCESS | Metrics & More | Article Recommendations | Supporting Information

ABSTRACT: Blood vessel damage resulting from trauma or diseases presents a serious risk of morbidity and mortality. Although synthetic vascular grafts have been successfully commercialized for clinical use, they are currently only readily available for large-diameter vessels (>6 mm). Small-diameter vessel (<6 mm) replacements, however, still present significant clinical challenges worldwide. The primary objective of this study is to create novel, tunable, small-diameter blood vessels with biomimetic two distinct cell layers [vascular endothelial cell (VEC) and vascular smooth muscle cell (VSMC)] using an advanced coaxial 3D-bioplotter platform. Specifically, the VSMCs were laden in the vessel wall and VECs grew in the lumen to mimic the natural composition of the blood vessel. First, a novel bioink consisting of VSMCs laden in gelatin methacryloyl (GelMA)/polyethylene(glycol)diacrylate/alginate and lyase was designed. This specific design is favorable for nutrient exchange in an ambient environment and simultaneously improves laden cell proliferation in the matrix pore without the space restriction inherent with substance encapsulation. In the vessel wall, the laden VSMCs steadily grew as the alginate was gradually degraded by lyase leaving more space for cell proliferation in matrices. Through computational fluid dynamics simulation, the vessel demonstrated significantly perfusable and mechanical properties under various flow velocities, flow viscosities, and temperature conditions. Moreover, both VSMCs in the scaffold matrix and VECs in the lumen steadily proliferated over time creating a significant two-cell-layered structure. Cell proliferation was confirmed visually through staining the markers of alpha-smooth muscle actin and cluster of differentiation 31, commonly tied to angiogenesis phenomena, in the vessel matrices and lumen, respectively. Furthermore, the results were confirmed quantitatively through gene analysis which suggested good angiogenesis expression in the blood vessels. This study demonstrated that the printed blood vessels with two distinct cell layers of VECs and VSMCs could be potential candidates for clinical small-diameter blood vessel replacement applications.

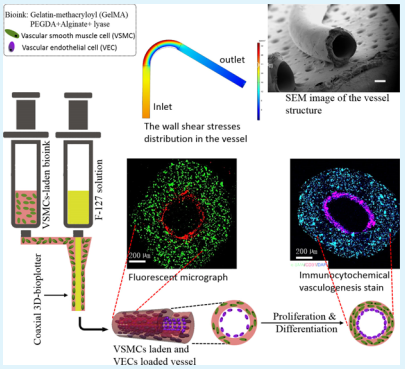

KEYWORDS: *3D bioprinting, small-diameter, blood vessel, smooth muscle, endothelium*

1. INTRODUCTION

Blood vessels are the most essential tissue in the human body, which transports blood cells, nutrients, oxygen, water, and other substances to the tissues throughout the body, and takes waste away. Blood vessel damage resulting from trauma or disease presents a serious risk of morbidity and even mortality globally. Maintaining the structural and functional integrity of blood vessels is crucial for large tissue survival throughout the body. Vascularization is always a prerequisite for complex tissue and organ regeneration.[1] After artificial replacement or replacement through allo/autologous donors, vascularization allows oxygen and nutrients to diffuse into the implants and then sustain cellular viability. It is crucial for the integrity and survival between the implant and the native tissue. With the significant advances in the field, synthetic vascular grafts have been successfully commercialized for clinical use (Dacron and Teflon).[2,3] Generally, the capillaries with 5−10 μm diameters do not need repair; they can spontaneously form through sprout vasculogenesis *in vivo*. Large-diameter vessels (>6 mm) are commercially available as an alternative to autologous vessels.[4] The small-diameter vessel (<6 mm) replacements, however, are still a significant clinical challenge worldwide.[5] The synthetic small-diameter vessels usually involve thrombosis and intimal hyperplasia caused by thrombogenicity between the synthetic surface and native vessel.[2] Therefore, fabricating biocompatible and biomimetic small-diameter blood vessels attracts tremendous attention globally.

There have been numerous attempts at fabricating small-diameter blood vessels, or tissue-engineered vascular grafts, by various tissue engineering methods including decellularized natural matrices,[6,7] electrospinning technique,[8−10] scaffold-

Received: August 18, 2020
Accepted: September 22, 2020
Published: October 2, 2020

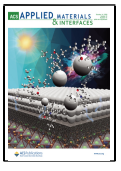

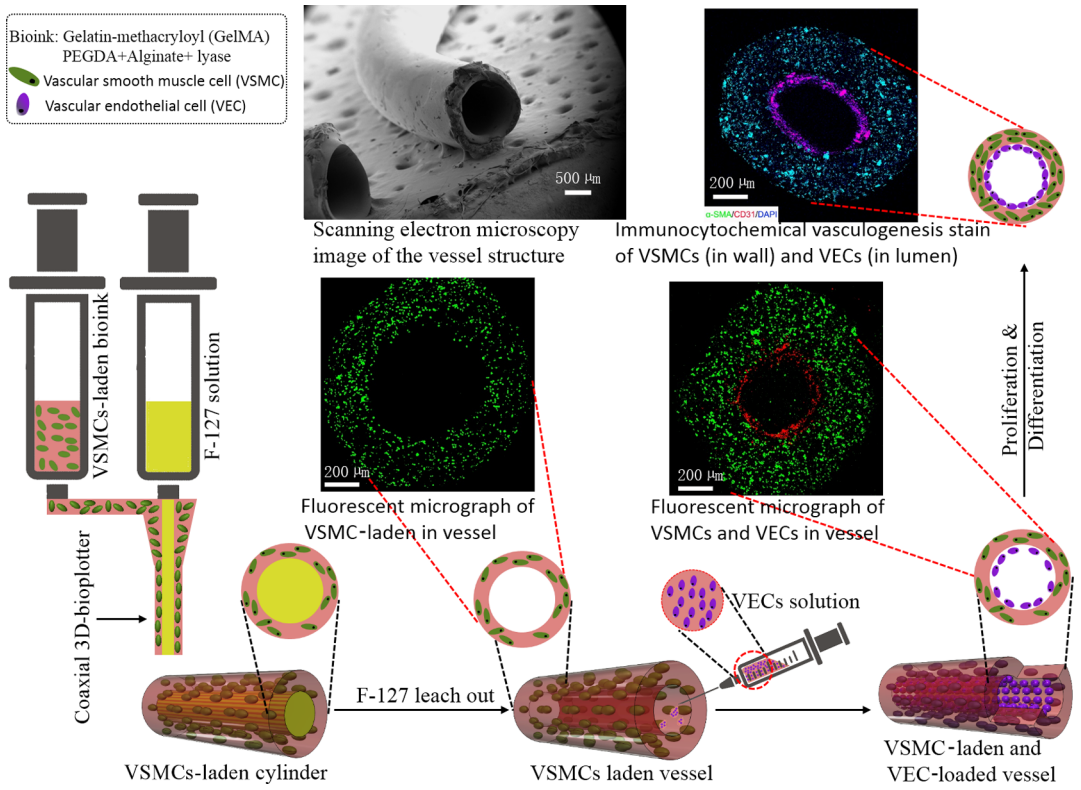

Figure 1. Schematic diagram of 3D bioprinting a biomimetic two-layer blood vessel.

based molding methods,[11−13] and so forth. Thus far, these conventional approaches are still not perfect with some complications, such as intricate decellularized processes, an unknown risk of immunological rejection, complex molding technological challenges, and so forth.[4,14] Some of these approaches only create monolayer endothelium lumen which was distinct from the structure of natural arteries and veins.[14] Moreover, engineering vascular grafts to biomimetic native tissue still presents challenges because of the complex hierarchical structure and composition of natural blood vessels.[14] Normally, the typical blood vessel is comprised three layers, the inner layer (tunica intima), the middle layer (tunica media), and the outer layer tunica adventitia). The thin inner layer consists of vascular endothelial cells (VECs) and connective tissue layers which are largely responsible for the exchange of substances. The thick middle layer consists of layers of smooth muscle supported by connective tissue responsible for structural maintenance. The outer layer mainly consists of connective fibers that join with perivascular nerves and surrounding tissues helping anchor vessels in their relative position.[3,6,15] Both VECs and vascular smooth muscle cells (VSMCs) play an essential role in maintaining the structural and functional integrity of blood vessels. VECs primarily take part in the maintenance of angiogenesis, proper hemostatic balance, vessel wall permeability (barrier function), and regulating blood flow.[16] SMCs mainly participate in structural support, mechanical regulation, regulation of blood circulation, hemodynamic behaviors, and other physiological activities.[17,18] The coordination and synergy between VECs and VSMCs are critical for maintaining the physiological function of natural blood vessels.

In recent years, conventional tissue engineering approaches are being revolutionized and promoted by advanced 3D printing technologies capable of fabricating customizable, hierarchical architecture in a layer-by-layer method with high precision and efficiency.[19−22] State-of-the-art 3D printing technologies have been used to fabricate vascular vessels[22,23] and can primarily be classified into several categories, including fused deposition modeling, digital light processing, stereolithography, extrusion-based, and droplet-based printing;[24,25] further variations between techniques are facilitated by various biomaterial selections. Considering the specific lumen structure of human blood vessels, an extrusion-based 3D bioprinter developed in our lab, where the nozzle was designed with a coaxial needle,[3,26] has shown promising results for our proposed blood vessel fabrication. This co-axial bioprinter can incorporate cells into the tunable ink and directly produce a tubular structure with a lumen through the extrusion-based platform. Therefore, this bioprinter will be used here to fabricate biomimetic blood vessels with biphasic cell layers.

In the past several decades, various synthetic and natural biomaterials have been employed to manufacture a variety of tissue-engineered vascular grafts.[25] In particular, the natural biomaterials have attracted more interests because of their excellent biocompatibility, biodegradability, and biosafety.[24] For instance, natural gelatin, alginate, and hyaluronic biomaterials are widely studied for tissue-engineered vascular graft fabrication.[3,22,23,27] In addition, synthetic materials [such as poly(vinyl alcohol), polylactic acid, polycaprolactone] also play a critical role in vascular tissue engineering because of their flexibility in design and tunable physical as well as chemical properties.[8,28] In the current study, in order to achieve excellent biocompatibility, mechanical properties and suitable printability, a biocompatible bioink with both natural and synthetic biomaterials [i.e., gelatin methacryloyl (GelMA), polyethylene-(glycol)diacrylate (PEGDA), and alginate] were prepared.

https://dx.doi.org/10.1021/acsami.0c14871
ACS Appl. Mater. Interfaces 2020, 12, 45904−45915

Specifically, GelMA, a proteinaceous derivative of gelatin, is a popular biomaterial and has been widely utilized for food, medicine, and pharmaceutical applications. Synthetic PEGDA is a biodegradable photopolymer and can improve the printability and mechanical strength of the printed scaffold.[20,29,30] Alginate derived from seaweed is also one popular natural biomaterial widely used in food, medical, and pharmaceutical fields.[31,32] All of these GelMA-, PEGDA-, and alginate-based hydrogels are able to incorporate living cells in order to fabricate biomimetic tissues.[20,31] Although these cell-laden strategies achieve impressive successes in tissue repair and regeneration, the growth and proliferation of laden cells were restricted because of surrounding hydrogel encapsulation. To address this problem, alginate lyase were introduced into our bioink to degrade the alginate and create sufficient spaces for further vascular cell growth. After breaking the space restriction of the surrounding hydrogels, it was expected that the laden cells can grow and proliferate faster.

Overall, the main objective of the study presented herein is to create novel biomimetic blood vessels with two distinct cell layers using VECs and VSMCs through an advanced 3D coaxial extrusion platform (Figure 1). The printing ink used in the current study was composed of GelMA, PEGDA, and alginate as well as alginate lyase. A VSMC-laden GelMA−PEGDA−alginate tube was first bioprinted and fabricated as a supporting middle layer, then the VECs were seeded in the lumen forming inner layers of the vessel-like matrix. The proliferation of VECs and VSMCs were investigated over different time intervals. Moreover, the relevant markers of vascular endothelial and smooth muscle cells [alpha-smooth muscle actin (α-SMA); the cluster of differentiation 31 (CD31), and von Willebrand factor (vWf)] were detected to evaluate the blood vessel generation using immunocytochemical analysis and real-time quantitative reverse transcription-polymerase chain reaction (RT-PCR) assays.

2. METHOD

2.1. Bioink Preparation. GelMA was synthesized as described in our previous reports.[20,26,29,30] Briefly, 10% (w/v) type-A gelatin (Sigma-Aldrich, USA) was fully dissolved into pure water with constant magnetic stirring at 60 °C for about 30 min. Methacrylic anhydride 4% (v/v) was added dropwise into the gelatin solution while continuously stirring at 50 °C for 2 h. Next, the reaction mixture was transferred into dialysis tubing (8−14 kDa cut-off) and was dialyzed against pure water to remove impurities at 40 °C for 5 days. Subsequently, the GelMA solution was fully lyophilized in a freeze dryer and the GelMA flock was harvested for subsequent experiments.

The bioink was prepared as follows. GelMA 10% (w/v), 1% (v/v) PEGDA750 (Sigma-Aldrich, USA), 1% (w/v) alginate (Sigma-Aldrich, USA), and 0.01% (w/v) alginate lyase (Sigma-Aldrich, USA) were dissolved into 1% (w/v) 2-hydroxy-4′-(2-hydroxyethoxy)-2-methylpropiophenone (Irgacure 2959, Sigma-Aldrich) solution. Irgacure 2959 is a photoinitiator that induces GelMA cross-linking under UV light. Prior to printing, the bioink was pre-warmed to 37 °C to avoid cells and lyase deactivation. All the components were dissolved with a phosphate-buffered saline (PBS) solution.

2.2. 3D Bioprinted Biomimetic Blood Vessels by a Coaxial 3D-Bioplotter. Biomimetic blood vessels were fabricated using our customized 3D extrusion-based bioprinter with a coaxial needle extrusion system.[3,26] This redesigned printer consists of a common 3D printer and a coaxial needle nozzle extrusion system which connects with two separate syringes for loading two types of bioinks. The syringe was simultaneously propelled by an electric motor controlled by the MatterControl software. The internal/external needle gauge can adjust to prepare the various sizes of vessels. In the current study, an internal needle diameter of 1.2 mm and an external needle diameter of 1.6 mm were selected for creating the vessel. Other parameters, including printing speed (1 mm/s) and extrusion flow rate (0.1 mL/s), were regulated and optimized for obtaining optimal print conditions. The printing procedures were executed at room temperature under a sterile environment. The detailed process was shown as follows.

A 20% (w/v) Pluronic F127 (Sigma-Aldrich, USA) solution was fed in one syringe connected with the internal needle (inner). The abovementioned bioink (10 wt % GelMA, 1% PEGDA, 1 wt % alginate, and 0.01 wt % alginate lyase in 1 wt % Irgacure 2959 PBS) containing VSMCs (1×10^6 cells/mL) was fed in another syringe connected with the external needle (outer). Next, the pre-warmed $CaCl_2$ solution (0.3 M) was placed on the z-control movable platform. Upon printing, a solid, wire-like vessel, consisting of a VSMC-laden outer layer and F127 inner core was fabricated by flowing out of the coaxial needle. The alginate vessel was ionically cross-linked when it came in contact with the ionic cross-linking $CaCl_2$ solution. After thirty seconds, the vessel was taken out and rinsed with PBS in order to remove the excess $CaCl_2$ solution. Next, it was exposed under a UV laser (355 nm) for 30 s to cross-link the GelMA/PEGDA the vessel. Subsequently, the vessel was placed in a medium with a constant gentle shake at 15 °C for 5 min to leach out the F127 inner core, revealing a tube-like vessel with a hollow core. In the current study, F127 was utilized as a sacrificial material for supporting construction and was then removed to generate a lumen structure. Finally, the VSMC-laden vessel with a lumen structure was created and then cultured in a VSMC growth medium at 37 °C, 5% CO_2, and 95% relative humidity.

After 2 h, the VECs, mixed with the growth medium containing 0.5% gelatin solution (1×10^6 cells/mL), were injected through the vessel lumen and then continuously incubated for 4 h. At predetermined time intervals, the vessel was flipped over and injected with the VEC−gelatin solution again following by incubation. This process was favorable for the uniform distribution of VECs in the lumen. After incubation, the VSMCs in the vessel wall were able to proliferate faster as an additional space was created as the alginate was gradually degraded by alginate lyase. At the same time, the VECs adhere and grow incrementally on the lumen with the incubation. Thus, fabricating a biomimetic blood vessel with two distinct cell layers of VSMCs and VECs.

2.3. Characterization of Printed Blood Vessels. The surface morphology of the vessel structure was observed by scanning electron microscopy (SEM, Zeiss NVision 40 FIB). The microporous structures of the bioink with or without alginate lyase were investigated for 6 days by SEM. The samples were sputter-coated with a 10 nm thick layer of gold and then characterized using a 5 kV electron beam. The perfusion effect of the printed vessel was tested by perfusing a colored solution through the vessel channel. In addition, mechanical properties of the vessel grafts were tested using an electromechanical universal testing machine (Applied Test Systems, Butler, USA) in the uniaxial tension mode at a rate of 8 mm/min. The slope of the stress−strain curves at 0−10% strain was calculated to evaluate the tensile modulus. The length of the sample was 10 mm.

https://dx.doi.org/10.1021/acsami.0c14871
ACS Appl. Mater. Interfaces 2020, 12, 45904−45915

2.4. Investigation of Fluid Flow through the Biomimetic Blood Vessel. PBS was simulated and utilized to perfuse the fabricated blood vessel. Two high precision microtemperature sensors were fixed on the inlet and outlet of the biomimetic blood vessel (10 cm) (Figure 3A). The temperatures of the two sites were real-time recorded using precision thermometers (Isotech TTI-22, USA). The PBS could be controllably heated and then pumped to perfuse the vessel at flow rates of 1 and 5 mL/min using a digital peristaltic pump (Masterflex, Cole-Parmer).[33] The temperature variation curve of the two sites at either end of the biomimetic blood vessel was recorded simultaneously under different flow velocities. The flow investigation was utilized to evaluate the feasibility of using the biomimetic blood vessel for fluid perfusion.

2.5. Investigation and Simulation of the Shear Stress on the Vessel Wall. The shear stress of blood vessel flow is generated by fluid flow across the lumen and it can be affected by many factors including vessel diameter, wall thickness, wall pressure, flow velocity, flow viscosity, and temperature. In the current study, the vessel diameter and wall thickness are fixed. Therefore, the shear stress on the vessel wall was investigated and simulated by regulating flow velocity, flow viscosity, and temperature. The flow velocity was perfused into the vessel at controlled flow rates ranging between 1 and 5 mL/min using a digital peristaltic pump. Flow viscosity (1−8 mPa s) was controlled by diluting the gelatin solution [0−6% (w/v)] with PBS (flow viscosity PBS was 1 mPa s). The fluid temperature (25−40 °C) was controlled by a water bath (Corning, USA). The average shear stress (τ) (dyn/cm^2) of the vessel was calculated using the Hagen−Poiseuille's law ($\tau = 4\eta Q/\pi r^3$). Where, ηWhs is the flow viscosity, Q is the flow velocity, and r is the vessel radius (0.5 mm). COMSOL Multiphysics (version 5.4) was employed to simulate the computational fluid dynamics (CFD) of the vessel. The Box−Behnken design[34] was applied to analyze the interactions among flow velocity, flow viscosity, and temperature on the average shear stresses of the vessel.

2.6. Vascular Cell Culture. Human VSMCs and human umbilical vascular endothelial cells (VECs) were purchased from American Type Culture Collection (ATCC) (PCS-100-021) and Thermo Fisher Scientific (C0035C), respectively. For VSMC proliferation, the cells were cultured in a growth medium which was composed of Medium 231 supplemented with the smooth muscle growth supplement. For VSMC differentiation, the cells were cultured in a differentiation medium which was composed of Medium 231 supplemented with the smooth muscle differentiation supplement. Unlike VSMCs, VEC is a type of mature cell that does not need to induce differentiation. VECs can be cultured in a human EC growth medium (211-500, Cell Applications). For the co-culture study, the blood vessels were cultured in a 1:1 mixed medium of the VEC growth medium and VSMC growth medium (or VSMC differentiation medium). All cells were incubated at 37 °C, 5% CO_2, and 95% relative humidity.

2.7. Laden VSMC Proliferation and Viability in the Bioprinted Vessel Structure. In order to visually monitor the laden VSMC proliferation in the printed vessel structure with or without alginate lyase, VSMCs were prestained with cell tracker and then cultured for 6 days. Before printing, VSMCs were harvested by routine procedures and then rinsed with PBS. Serum-free medium, containing 20 μM CellTracker Green CMFDA (Thermo Fisher Scientific, USA), was added and mixed with VSMCs and incubated for 45 min in an incubator.[20] Next, cells were collected by centrifugation and rinsed twice with PBS to remove excess cell trackers. After that, the pre-labeled VSEMCs were suspended and mixed into the bioink for printing. At predetermined time intervals (1 day, 3 days, and 6 days), the cross section of the vessel structure was observed per the manufacturer's instruction by a laser confocal microscope (Carl Zeiss LSM 710).

Meanwhile, the cell count method was employed to evaluate the laden VSMC proliferation in the vessel structures with or without alginate lyase. Briefly, at the predetermined time interval, the culture medium of the vessel structure was replaced with a fresh medium containing 10% CCK-8 solution (Dojindo, Japan) and continuously incubated for 8 h. Next, 100 μL of the culture medium was transferred into a 96-well plate. The absorbance was measured by a spectrophotometer (Thermo, USA) at a wavelength of 450 nm.

Furthermore, a Live−Dead cell staining kit (BioVision, Inc.)[20] was used to investigate the laden VSMC viability in the vessel structure. At the predetermined time interval, the vessel structure was taken out and incubated in a free medium containing calcein-AM (2 μM) and propidium iodide (4 μM), and continuously incubated for 1 h. After incubation, the cross section of the vessel structure was observed per the manufacturer's instruction using a laser confocal microscope.

2.8. Observation of the Bioprinted Blood Vessel with Two Cell Layers of VSMCs and VECs. In order to visually monitor the two cell layers of VSMCs and VECs in the blood vessel structure, the VSMCs and VECs were pre-stained with different cell trackers and then co-cultured for 6 days. As abovementioned, VSMCs and VECs were harvested by routine procedures and then rinsed with PBS. Subsequently, VSMCs and VECs were pre-labeled by CellTracker Green CMFDA and CellTracker Orange CMTMR Dye (Thermo Fisher Scientific Inc.). Next, the green-labeled VSEMCs were suspended and mixed into the bioink for printing the vessel well, and the red-labeled VECs were suspended and injected through the vessel lumen as discussed in Section 2.2. Finally, the cross section of the vessel structure was imaged per the manufacturer's instruction using a laser confocal microscope at each of the predetermined time intervals (1 day, 3 days, and 6 days).

2.9. Vasculogenesis Immunostaining of the Blood Vessel Structure. Immunostaining was performed to evaluate the bioactivity of VSMCs and VECs in the blood vessel structure. The α-SMA of VSMCs and CD31 of VECs were evaluated. After 3-day culture of the vessels with two cell layers of VSMCs and VECs, the co-culture media (VEC medium + VSMC growth medium) were replaced by a mixed medium (1:1) of VEC medium and VSMC differentiation medium, nd followed by continuously 21 day culture. Then, the samples were collected, rinsed with PBS, and fixed in 10% formalin for 20 min. Next, they were permeabilized in 0.2% Triton X-100 solution for 30 min at room temperature. Then, the vessel structures were incubated with a blocking solution [consist of 1 wt % bovine serum albumin and 22.52 mg/mL glycine in PBST (PBS + 0.1 wt % Tween 20)] for 3 h to block the unspecific binding of the antibodies. Both recombinant anti-α-SMA antibody (Alexa Fluor 488) (ab202295, Abcam) and anti-CD31 antibody (ab28364, Abcam) were diluted with PBST containing 1% BSA at a ratio of 1:500. Then, the vessel structure was incubated in the antibody solution away from light at 4 °C for 48 h. Subsequently, the goat anti-rabbit IgG H&L (Alexa Fluor 647, ab150079, Abcam) was diluted with PBST, containing 1% BSA, at a ratio of 1:200 as secondary antibodies. After rinsing with PBS, the vessel structure was incubated in the secondary

https://dx.doi.org/10.1021/acsami.0c14871
ACS Appl. Mater. Interfaces 2020, 12, 45904−45915

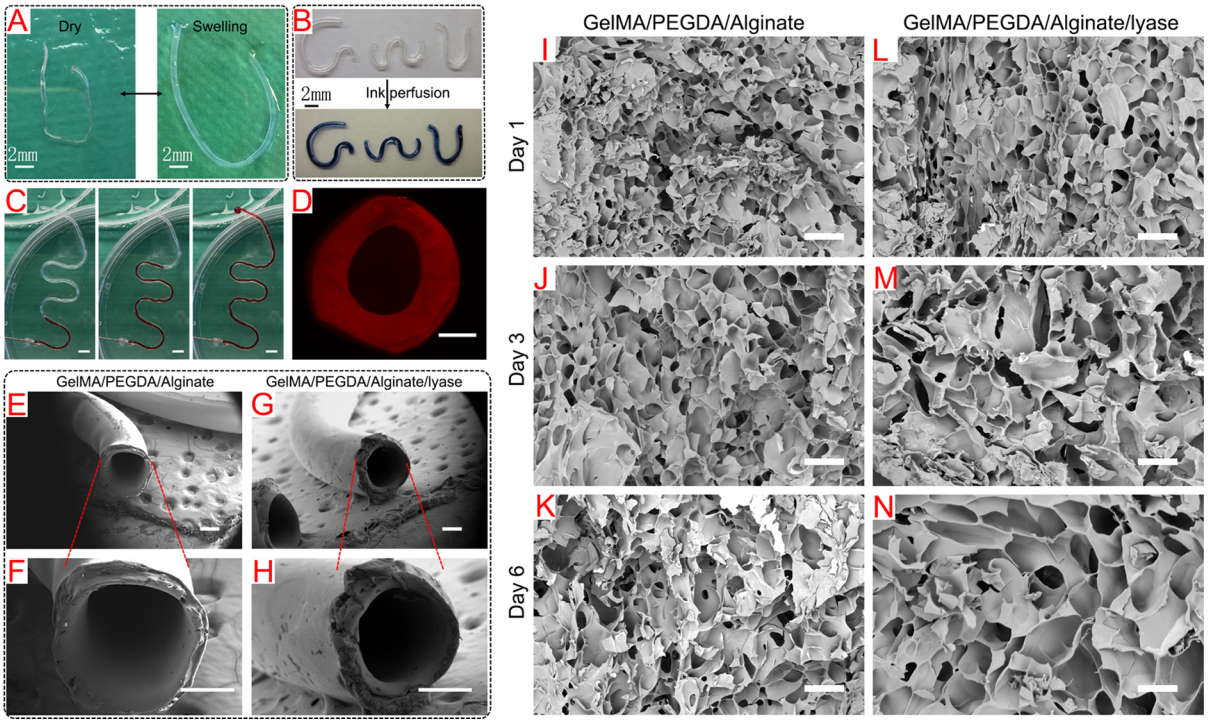

Figure 2. Morphologies of 3D bioprinted biomimetic blood vessels. (A) Vessel remained intact through both the swelling and dry status. Vessels perfused with (B) the blue and (C) red ink fluid. Scale bar = 5 mm. The inner diameter of the vessel was about 1 mm. Fluorescence micrographs (Rhodamine B) in a cross-sectional view (D) of the vessel structure. Scale bar = 300 μm. SEM images of the blood vessel structure (E,F) without and (G,H) with a lyase composition. Scale bar = 500 μm. SEM images of the cross-section of bioprinted blood vessels (I−K) without and (L−N) with lyase in 6 days. Scale bar = 100 μm. The porous structures were generated and more spaces were produced for laden cell propagation after alginate was gradually degraded by lyase over time.

antibody away from light at 4 °C for 4 h. Finally, the sample was incubated in 4,6-diamidino-2-phenylindole (DAPI) solution (1%) for 10 min. In this experiment, the samples were rinsed three times with PBS before moving on to the next step. The immunostaining images were recorded using a laser confocal microscope.

2.10. Gene Analysis. The gene expression involved in vasculogenesis (vWf, CD31, and α-SMA) was quantitatively analyzed by an RT-PCR assay. As above-mentioned, vessels with VSMCs and VECs were cultured for 3 days in the mixed growth medium of VEC medium + VSMC growth medium. After that, the growth medium was replaced by a mixed differentiation medium of VEC medium + VSMC differentiation medium. In order to investigate the relevant gene expression of vessel vasculogenesis, the vessel with VSMCs and VECs cultured in a mixed growth medium was chosen as the control group. After one week of culture, the vessel structures were treated with TRIzol reagent and then the total RNA was exacted by the classical chloroform method. The quantity and purity of RNA were determined by the OD 260/280 nm assay (1.8−2.0) using NanoVue Plus (Biochrom, Ltd. USA). The complementary DNA (cDNA) was synthesized using the PrimeScript RT Master Mix kit (Takara). The CFX384 Real-Time System (Bio-Rad, USA) and SYBR Premix Ex Taq II kit (Takara) were utilized to perform RT-PCR analysis per the manufacturer's protocol. Glyceraldehyde 3-phosphate dehydrogenase (GAPDH) was used as the endogenous housekeeping gene. Each sample was analyzed in triplicate. The relative gene expression was normalized and calculated using a standard 2-delta delta cycle-threshold ($2^{-(\Delta\Delta Ct)}$) method. The sequences of primers for α-SMA, vWf (a blood glycoprotein), CD31, and GAPDH are shown as follows.[3] α-SMA: Forward primer 5′-CTGGGGTATTGGGGGCATC-3′ and reverse primer 5′-CTGTTCCAGCCATCCTTCAT-3′. vWf: Forward primer 5′-CACCATTCAGCTAAGAGGAGG-3′ and reverse primer 5′-GCCCTGGCAGTAGTGGATA-3′. CD31: Forward primer 5′-GAGTCCTGCTGACCCTTCTG-3′ and reverse primer 5′-CACTCCTTCCACCAACACCT-3′. GAPDH: Forward primer 5′-GGAGCGAGATCCCTCCAAA-3′ and reverse primer 5′-GGCTCCCCCCTGCAAA-3′.

2.11. Statistical Analysis. All the data were presented as the mean ± standard deviation. Statistical analysis was performed by one-way ANOVA method. The level of $p < 0.05$ was considered as statistically significant in experimental data.

3. RESULTS AND DISCUSSIONS

3.1. 3D Bioprinted Small Diameter Blood Vessel and Characterization. The bioprinted blood vessel was successfully fabricated *via* our advanced 3D coaxial extrusion platform (Figure 1). The morphology and physical characterizations are shown in Figure 2. The blood vessel is still robust after drying and swelling in PBS several times (Figure 2A). Vessels with various lengths or curves all perfused smoothly with color inks (Figure 2B,C and Supporting Information S1). The fluorescence micrographs of the blood vessel wall and lumen in a cross-sectional view are shown in Figure 2D. The thickness of the wall and the diameter of the lumen are about 0.3 and 1 mm, respectively. The SEM images of the blood vessel structure without and with lyase are shown in Figure 2E−H. A tube-like vessel was fabricated, but no significant differences were observed between the vessel structure without and with lyase because alginate lyase did not influence vessel fabrication. In the

https://dx.doi.org/10.1021/acsami.0c14871
ACS Appl. Mater. Interfaces 2020, 12, 45904−45915

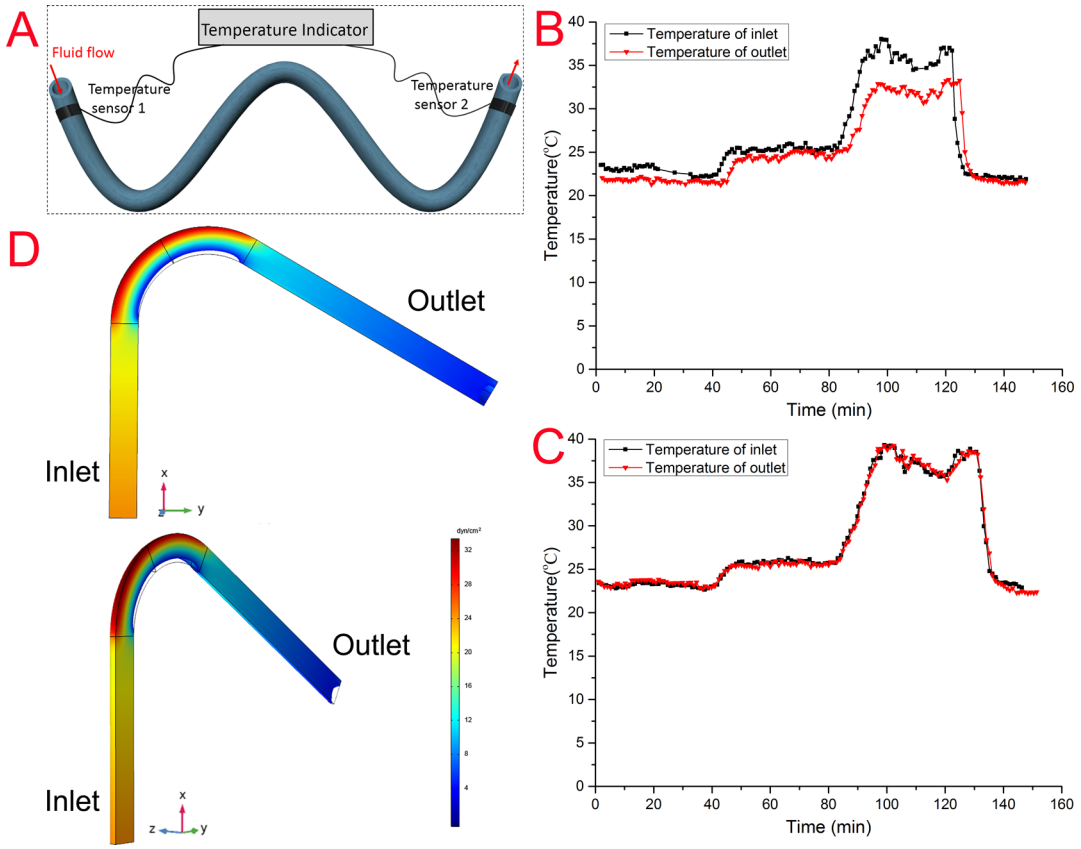

Figure 3. (A) Schematic diagram of temperature detection in the biomimetic blood vessel. The temperatures of the inlet and outlet could be monitored by a temperature recorder. The temperature variation curve of the inlet and outlet of the biomimetic blood vessel when perfusing different flow velocities (B) 1 and (C) 5 mL/min. (D) The wall shear stresses distribution in the vessel.

3D coaxial extrusion system, the outer syringe was fed with GelMA/PEGDA/alginate/lyase ink and the inner syringe was fed with the F127 solution. After printing, the solid, wire-like vessel consists of a GelMA/PEGDA/alginate/lyase outer layer and an F127 inner core created after cross-linking first by calcium ionic exposure followed by UV light. The sacrificial material, F127, was utilized to support the vessel shape. Subsequently, the inner F127 core was easily leached out at 15 °C because of its unique features of a solid status above 30 °C and solution status below 20 °C. Finally, a small diameter blood vessel with a lumen structure was successfully produced as expected.

Porous structures were observed in both matrices, without and with lyase (Figure 2I–N) because of the inherent hydrogel-based structure, which benefits nutrient storage and exchange for cell growth and proliferation.[30,35] With alginate lyase introduction, the hydrogel morphologies of GelMA–PEGDA–alginate have some significant changes between them (Figure 2K,N). The pores in GelMA/PEGDA/alginate/lyase matrices (Figure 2M,N) are more porous than GelMA/PEGDA/alginate matrices (Figure 2J,K) after 3 and 6 days, which could be explained by the gradual degradation of alginate with lyase. This degradation process is favorable for nutrient exchange with the ambient environment and simultaneously leaving more space for laden cell propagation in matrices. Alginate lyase was considered for degrading alginate by cleaving the glycosidic bond *via* a β-elimination mechanism. In addition, it involved saccharification of the acidic polysaccharides for the production of bioethanol which may have latent toxicity to cells.[36] In order to investigate the cytotoxicity of alginate lyase and optimize the proper concentration, VSMCs were cultured with different concentrations of alginate lyase for 72 h. The VSMC proliferation is shown in Figure S1. The result illustrated that the VSMC growth was affected when the concentrations were higher than 0.02 mg/mL. The cell growth in 0.01 and 0.02 mg/mL groups had no significant influence when compared with the control group. The phenomenon implied that the alginate lyase with a high concentration might have latent cytotoxicity. Finally, an optimal concentration of 0.01 mg/mL was determined to be used in the current study after evaluation.

The primary ink consists of GelMA (10%), PEGDA (1%), and alginate (1%) as well as alginate lyase (0.01%). With the assistance of a photoinitiator (I2959), the GelMA and alginate can be cross-linked under UV light. The alginate can be ionically cross-linked by Ca^{2+} when the vessel flows out and comes in contact with the $CaCl_2$ solution. A combination of the GelMA, PEGDA, and alginate ultimately created the vessel structures in the current study. Although alginate will be gradually degraded by alginate lyase, the main architecture will be maintained by the small amount of cross-linked PEGDA. As such, the diminishing volume of alginate in the ink will not weaken the structure. The function of alginate in the bioink is to generate porous structures, leaving spaces for cell proliferation. This design fully considered the space restriction challenges resulting from hydrogel encapsulation, which broadly existed in previous cell-laden strategies. By introducing the lyase, the laden cells are able to grow and proliferate faster as a result of the increase in space.

The Young's modulus and mechanical nonlinear stress–strain curve property of the bioprinted blood vessels is shown in Figure S2. The tension modulus, within the range of 0.2–1 MPa, could

https://dx.doi.org/10.1021/acsami.0c14871
ACS Appl. Mater. Interfaces 2020, 12, 45904–45915

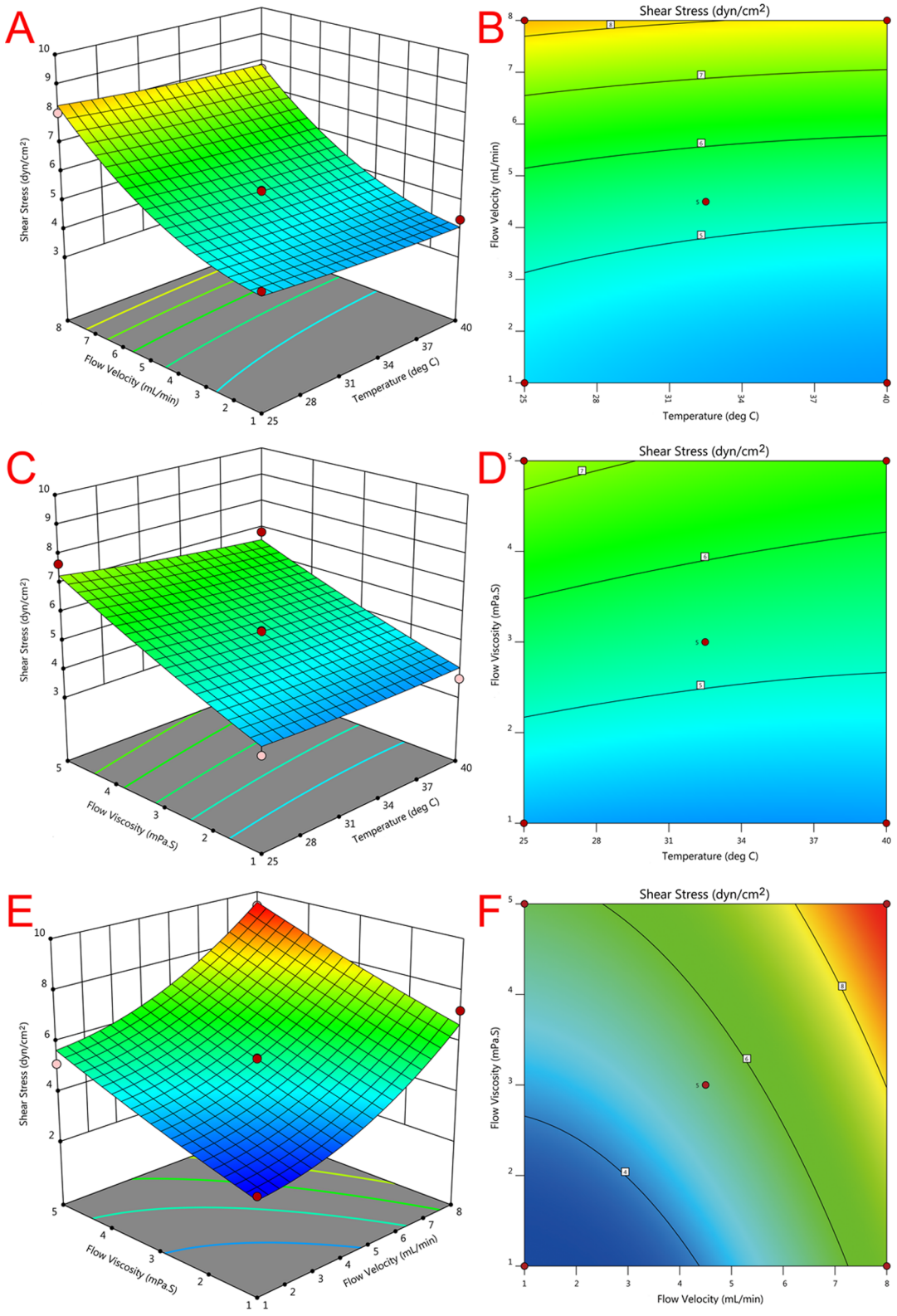

Figure 4. Response surface plot (A) and corresponding contour plane plot (B) for the effect of flow velocity and temperature on shear stress. Response surface plot (C) and corresponding contour plane plot (D) for the effect of flow viscosity and temperature on shear stress. Response surface plot (E) and corresponding contour plane plot (F) for the effect of flow viscosity and flow velocity on shear stress. These plots reflect the interaction among flow velocity, flow viscosity, and temperature on the average shear stresses of vessels.

be considered as two regions: low and high strain regions which are similar to the literature's reports.[37,38] Pure GelMA or alginate hydrogel at low concentrations lacked sufficient mechanical stress. Proper PEGDA incorporation could improve the printability and mechanical strength of the vessel. The modulus range allows fluid to pass through the small-diameter vessel.

3.2. Temperature Variation of Fluid Flow through the Bioprinted Blood Vessel. In order to simplistically investigate

https://dx.doi.org/10.1021/acsami.0c14871
ACS Appl. Mater. Interfaces 2020, 12, 45904−45915

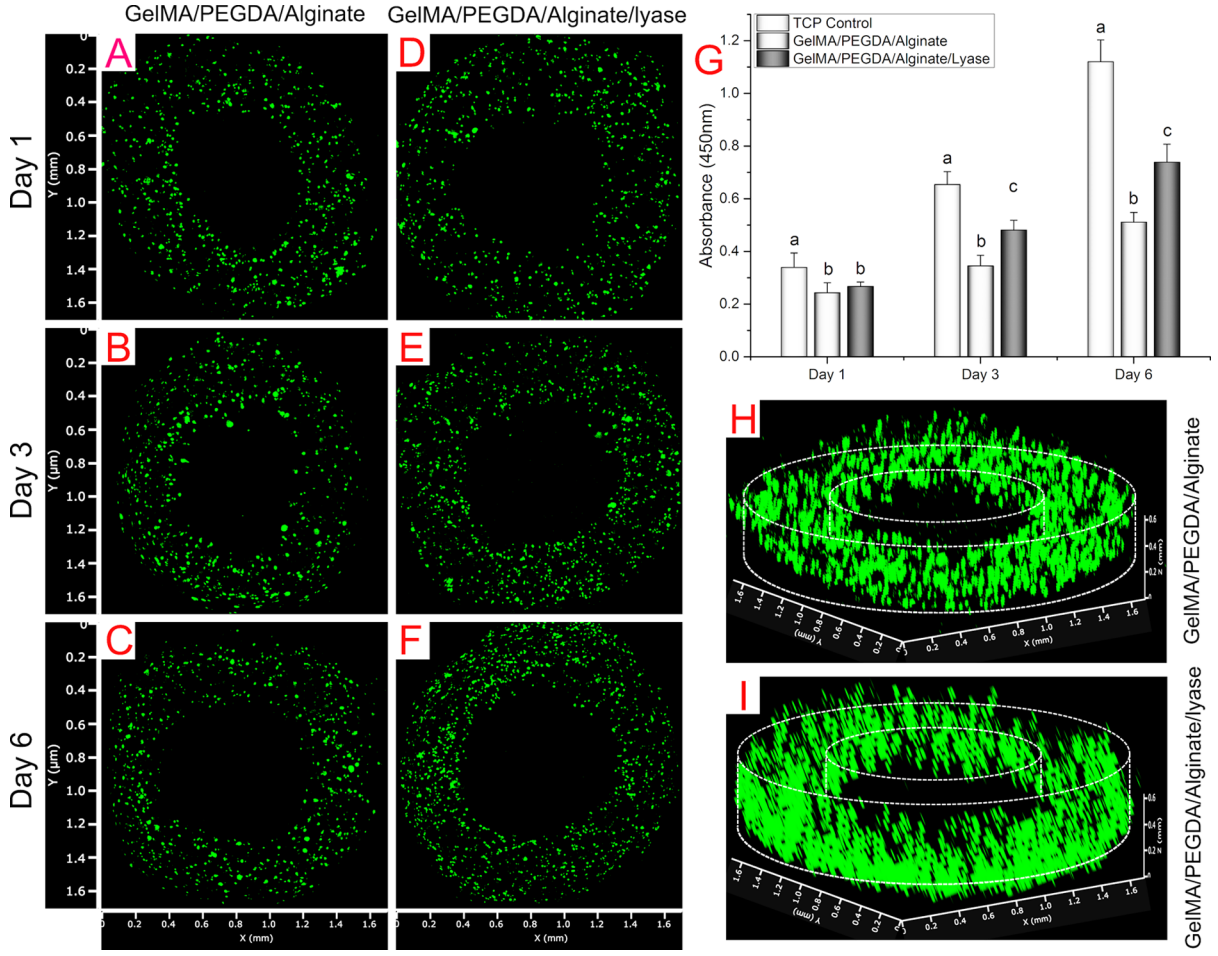

Figure 5. Confocal fluorescent micrographs in a cross-sectional view of VSMCs in vessels (A−C) without and (D−F) with lyase after 1, 3, and 6 days. VSMCs were prestained by Cell Tracker Green CMFDA dye (green). (G) Corresponding proliferation of VSMCs in vessels without and with lyase at 6 days. Data are the mean ± standard deviation; $n = 8$. The same letter indicates no difference at the same time point. The fluorescent micrographs inside view of VSMCs in vessels (H) without and (I) with lyase at 6 days.

the feasibility of the biomimetic blood vessel use for fluid perfusion, the PBS was perfused into the vessel with different flow rates ranging from 1 to 5 mL/min. The schematic process for the recording temperature is shown in Figure 3A. The temperature variation curves of the inlet and outlet in the biomimetic blood vessel are shown in Figure 3B,C. When PBS with different temperatures (23−37 °C) was pumped into the vessel with flow rates of 1 or 5 mL/min, inlet and outlet sensors successfully recorded the temperature variations. Moreover, the temperature variation curves in the inlet and outlet sites have a similar variation tendency. However, the results (Figure 3B) showed that the temperature at the outlet was slightly lower than that of the inlet at each time point after perfusing at 1 mL/min. Comparatively, no temperature differences were observed at the inlet and outlet sites for each time point after perfusing at 5 mL/min (Figure 3C). The phenomenon could be explained by the fact that, when perfusing at 1 mL/min, the temperature of PBS gradually dropped when fluid slowly flowed from the inlet to the outlet because the vessel was exposed to the surrounding atmosphere and the heat was being released to the ambient environment. Nevertheless, when perfusing at 5 mL/min, the fluid flowed comparatively fast from the inlet to outlet, less heat of fluid was lost to the ambient environment, and the temperatures at the inlet and the outlet had little change. Furthermore, the temperature variation at the two sites demonstrated high similarity which implied the bioprinted blood vessel has potential feasibility for fluid perfusion.

3.3. Simulation Analysis of the Shear Stress on the Vessel Wall. Because the vessel exhibited significant perfusion properties, the CFD of the vessel were simulated simplistically. The wall shear stress distribution of the vessel is shown in Figure 3D. The shear stresses of regions gradually enhanced from the inlet to bending areas and then relieved on outlet areas. The maximum values were evident in bending areas which is consistent with natural phenomena. In order to investigate the structural integrity and function of the biomimetic vessel, the effect of various factors (flow velocity, flow viscosity, and temperature) on the average shear stresses of the vessel were evaluated under different conditions. The response surface plot and the contour plane plot for the effect of flow velocity, flow viscosity, and temperature on shear stress is shown in Figure 4. We found that shear stress increased with the increase of flow velocity (Figure 4A,E) and flow viscosity (Figure 4C,E). However, the shear stress slightly decreased with an increase in temperature (Figure 4A,C), while the rangeability of shear stress was not significantly different when compared with the other two factors. The results demonstrated that flow velocity and flow viscosity can affect the shear stress of the vessel. Moreover, the first two factors have more positive effects compared with the last one in the defined range. In the current

https://dx.doi.org/10.1021/acsami.0c14871
ACS Appl. Mater. Interfaces 2020, 12, 45904−45915

study, the vessel diameter and wall thickness are fixed. High flow velocity induced more fluid through the vessel lumen resulting in excess shear stress on the vessel surface. Furthermore, high flow viscosity led to an increase of fluid resistance in the lumen, and it also resulted in more shear stress on the vessel surface. Interestingly, high temperatures could increase flow velocity and decrease flow viscosity. Thus, the temperature increase might induce an increase or decrease of shear stress that depends on which factor had prior influence. In the current study, the shear stress slightly decreased with an increase of temperature that means flow viscosity had a narrow margin overflow velocity; however, the priority lacked statistical difference. Nevertheless, the phenomena indicated that all factors, flow velocity, flow viscosity, and temperature, could influence shear stress, and they have complex interactions among them which were similar to the sophisticated conditions present *in vivo*.[39] In order to evaluate the vessel property under rigid conditions, value ranges of factors, 1−5 mL/min for velocity, 1−8 mPa s for viscosity, and 25−40 °C for temperature were selected far from the normal physiological conditions. In a native blood vessel, the shear stress of the vessel increases with the velocity and/or viscosity raising of blood fluid. In addition, the shear stress will recover to normal when the velocity and/or viscosity of blood fluid decrease because of the excellent elasticity property of the blood vessel. In the current study, the printed vessel perfused various rigid fluids and demonstrated corresponding shear stresses which were considered to have a similar elasticity property of real blood vessels. It suggested that the biomimetic printed vessel can sustain blood vessel function. These results indicated that the vessel possesses relevant mechanical properties to carry the fluid flow and exhibits great potential for future blood vessel replacement.

3.4. Proliferation and Viability of VSMCs in the Vessel. To visually observe the laden VSMC growth in vessels with or without lyase, VSMCs were pre-stained with a green cell tracker and monitored for 6 days. The fluorescent micrographs in the cross-sectional view of VSMCs are shown in Figure 5A−F,H,I. Either with or without lyase, the cells uniformly distributed in matrices and gradually grew with time. However, the cell amount in the vessels with lyase exceeded that of those without lyase after 3 and 6 days (Figure 5B,C,E,F). The observation was also confirmed by the quantitative analysis results as shown in Figure 5G. The cell densities in the lyase group increased by 39.4 and 44.6% when compared with that without lyase at 3 and 6 days, respectively. The results indicated that the laden VSMCs proliferated faster in the lyase group. As aforementioned, with the alginate gradual degradation, more spaces were produced that enhanced nutrient exchange with an ambient environment. Moreover, the laden cells were allowed to grow steadily in the matrix pores without space restriction. These results are consistent with design expectations.

The viability of VSMCs in vessels is investigated for 6 days by a live−dead staining method and shown in Figure 6. The result elucidated that most of VSMCs were alive (green color) and proliferated well in the matrix over time despite some dead cells (red color) occurring at the initial time point (Figure 6A−C). After 6 days, the live cells distributed in the matrix (Figure 6D,F), which indicated that the calcium ionic and UV cross-linking did not inhibit cell proliferation. Upon bioprinting, the solid wire-like vessel consisting of VSMC-laden GelMA/PEGDA/alginate/lyase (outer layer) and F127 (inner core) was fabricated from the co-axial needle. The alginate in the matrix was cross-linked upon contacting a $CaCl_2$ solution.

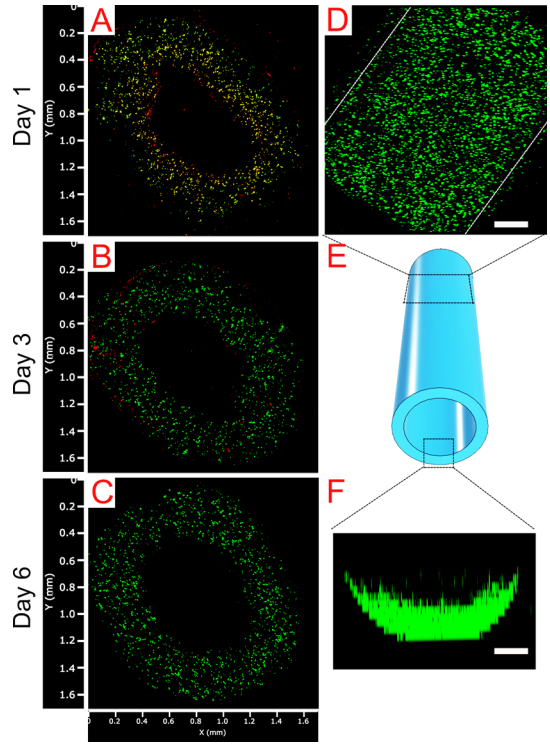

Figure 6. Confocal fluorescent micrographs in a cross-sectional view of VSMCs in the vessel with lyase after 1 (A), 3 (B), and 6 (C) days. At each time point, the live and dead cells were stained by calcein-AM (green) and propidium iodide (red), respectively. The fluorescent micrographs in (D) top view and (F) side view of VSMCs in the vessel with lyase at 6 days. Scale bar = 200 μm. (E) Schematic illustration of the bioprinted blood vessel structure. The results indicated that the cell viability steadily increased with the incubation time which suggested the cell activity gradually restored.

Subsequently, the GelMA/PEGDA in the matrix was cross-linked when exposed under UV light. On day one, a lower cell viability was observed and exhibited red or yellow color because of the certain effect of cross-linking factors. However, the cell viability steadily increased with the incubation time which suggested that the cell activity gradually restored after three days of culture. Although the $CaCl_2$ solution and UV light are considered as adverse effects harming cells, their negative influences only restrict in over dosage or over range situations. The security and reliability of the $CaCl_2$ solution and UV light in the appropriate range have been proven previously.[3,20,31] In the current study, the viabilities of laden cells after being exposed to calcium ionic for 30 s and under UV light for 30 s are still higher which confirmed the feasibility of our design.

3.5. Observation of the Bioprinted Vessel Structure with Two Cell Layers of VSMCs and VECs. To visually monitor the two cells' behavior in the vessel, VSMCs and VECs were separately pre-stained with green and red cell tracker and monitored for 6 days. The fluorescent micrographs in the cross-sectional view of VSMCs and VECs are shown in Figure 7. The VSMCs in the matrix and VECs in the lumen both steadily proliferated over time. In the previous experiments, the VEC solution was directly injected and perfused through the vessel lumen. However, it was found that most of the VEC solution passed through the vessel and dispersed in the medium; only a few remained in the lumen because of substance diffusion in the medium. To address this issue, VECs were first mixed with medium containing 0.5% gelatin and then injected into the

https://dx.doi.org/10.1021/acsami.0c14871
ACS Appl. Mater. Interfaces 2020, 12, 45904−45915

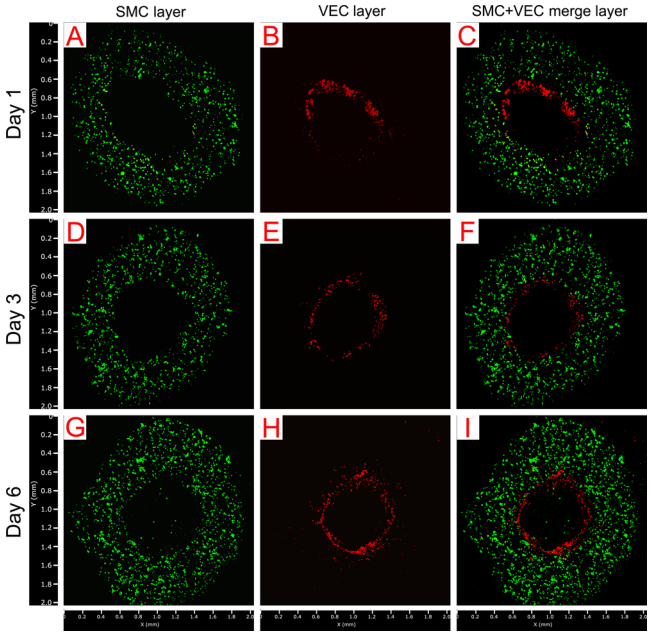

Figure 7. Confocal fluorescent micrographs in the cross-sectional view of VSMCs (in the wall) and VECs (in lumen) co-cultured after 1, 3, and 6 days. Fluorescent micrographs of the VSMC layer (A,D,G), VEC layer (B,E,H), and the merged two layers (C,F,I) on day 1, 3, and 6, respectively. VSMCs and VECs were pre-stained by Cell Tracker Green CMFDA dye (green) and Orange CMTMR dye (red), respectively. The results indicated that both VSMCs in the matrix and VECs in the lumen proliferated steadily over time.

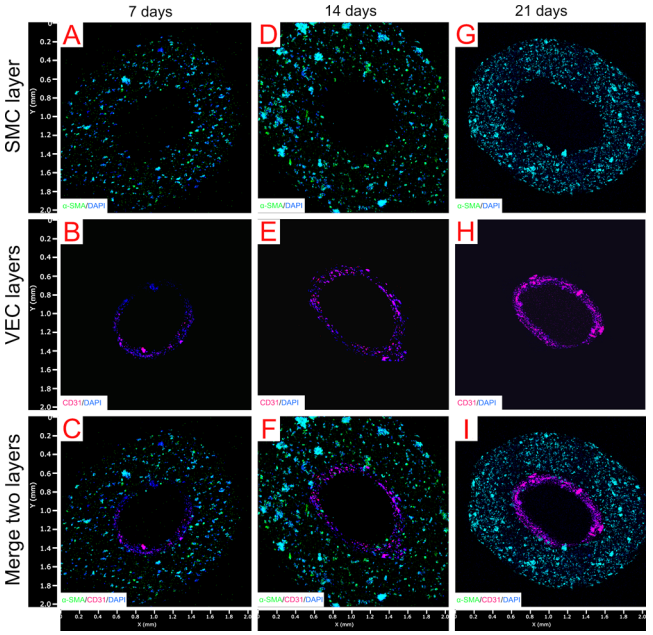

Figure 8. Immunocytochemical stain of vasculogenesis in a cross-sectional view of VSMCs (in the wall) and VECs (in the lumen) co-cultured after three weeks. Fluorescent micrographs of the VSMC layer (A,D,G), VEC ladyer (B,E,H), and the merged two layers (C,F,I) on weeks 1, 2, and 3, respectively. The specific marker of mature smooth muscle and endothelium, as well as cell nuclei, were stained by α-SMA (green), CD31 (red), and DAPI (blue), respectively. Results suggested vascular smooth muscle maturation and angiogenesis of blood vessels with biomimetic two cell layers.

lumen followed by incubation. These strategies are favorable for uniform deposition of VECs in the lumen. First, a certain amount of gelatin mixture into the medium was able to increase the solution viscosity which effectively slowed down the process of substance diffusion into the ambient medium and prolonged the VEC retention in the lumen. Second, flipping over the vessel after 4 h of incubation and re-injecting the new VEC medium was favorable for VECs uniformly depositing throughout the whole lumen. Finally, both VSMCs and VECs were distributed in the vessel matrix and lumen through these strategies, which was confirmed by the current results.

In the native blood vessel, the common blood vessel is comprised three layers, the inner, the middle, and the outer layers. The middle layer, including VSMCs and connective tissue, is much thicker than the inner layer composed by the VEC monolayer. Although the current design of the VSMC and VEC layers are not exactly the same as the natural ones. It can efficiently promote cell viability and maintain sufficient mechanical/elastic strength when perfused through by rigid fluid conditions.

3.6. Immunostaining and Quantitative Analysis of Vasculogenesis. The immunocytochemistry and morphocytology of vasculogenesis were recorded after three weeks (Figure 8). The α-SMA and CD31 antibodies were selected as specific VSMC and VEC biomarkers, respectively. Both α-SMA (green) and CD31 (red) stainings in the matrix and lumen were enhanced over time which demonstrated that the mature α-SMA and platelet endothelial cell adhesion molecules were expressed successfully. α-SMA (an actin isoform) predominates within VSMCs and plays a role in a blood vessel and fibroblast contractility.[40] The α-actin phenotype of smooth muscle is involved in the fabrication and integrity of the vessel structure. Moreover, the α-SMA phenotype is highly related to cell motility and the contractile apparatus of active cells. CD31 is a constituent of the endothelial intercellular junction and plays a major role in the adhesion cascade between VECs during angiogenesis.[41] CD31 is involved in several functions, including transendothelial migration of leukocytes, angiogenesis, and integrin activation. The α-SMA and CD31 expressed in the vessel structure implied that vascularization was generated after 7 days, which was also confirmed by quantitative analysis of the RT-PCR assay as discussed below.

Three cell-specific gene markers (α-SMA, vWf, and CD31) were employed for evaluating the vasculogenesis of the vessel structure. The relative gene expressions of α-SMA, vWf, and CD31 were quantitatively determined by RT-PCR using GAPDH as an endogenous housekeeping gene (Figure 9). The gene expression α-SMA increased 5.4-fold when compared with the growth supplement group. The vWf and CD31 gene expression did not show a significant difference between the growth supplement and differentiation group. VSMCs need to be cultured in a differentiation medium to enhance the expression amounts of smooth muscle α-actin which is involved in the fabrication and integrity of the vessel structure. Nevertheless, the VECs did not need to be inducted into differentiation and they could intrinsically express vWf and CD31 in proper cultural conditions. Therefore, the results indicated that the vasculogenesis and vascular maturation had been enhanced in the vessel. The α-SMA gene in vascular smooth muscle produced smooth muscle actin and participated in vasculogenesis. The vWf and CD31 gene were also involved in the angiogenesis of endothelial function. VWF is a blood glycoprotein presented in the endothelium, megakaryocytes,

https://dx.doi.org/10.1021/acsami.0c14871
ACS Appl. Mater. Interfaces 2020, 12, 45904−45915

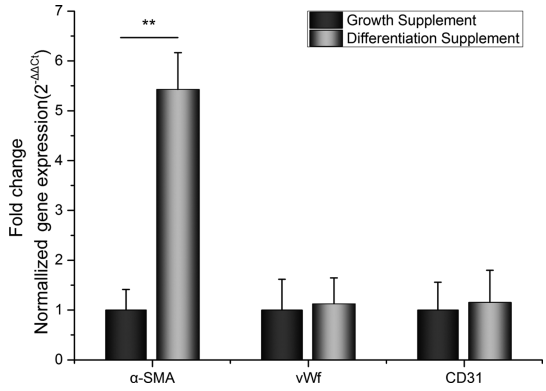

Figure 9. Normalized gene expression (α-SMA, vWf, and CD31) of growth and differentiation group by the RT-PCR assay after one week. The experiments were repeated three times. Data are presented as the mean ± standard deviation, $n = 8$. $^{**}p < 0.01$ when compared to control groups. Results suggested the vessel significantly expressed vascular smooth-muscle actin after one-week differentiation. At the same time, the vWf, and CD31 expressions in both groups implied that the vasculogenesis of bioprinted blood vessels initiated after endothelial seeding in the vessel.

and subendothelial connective tissue.[42] If its expression is deficient, it will result in many diseases, including thrombotic thrombocytopenic purpura, Heyde's syndrome, and hemolytic–uremic syndrome.[43] The resultant phenomena illustrated that both VSMCs and VECs have higher bioactivity and involved vasculogenesis which is consistent with the aforementioned immunostaining results. The bioprinted vessel with two cell-layers of VSMCs and VECs could be a valuable potential small-diameter vasculature replacement in the clinic.

4. CONCLUSIONS

In summary, a biomimetic blood vessel consisting of VSMCs (laden in the wall) and VECs (seeded in the lumen) was successfully created by a 3D coaxial bioprinting platform. Considering the space restriction issues for laden cell growth, lyase was introduced into the bioink for gradually degrading alginate of GelMA/PEGDA/alginate matrices. This specific design is favorable for nutrient exchange with the ambient environment and simultaneously leaves more space for laden cell propagation in matrices. This vessel exhibited a tube-like shape and could be perfused through the lumen with fluid. The vessel demonstrated significant perfusable properties under various conditions of flow velocity, flow viscosity, and temperature. The laden VSMCs grew faster in the lyase group than that without the lyase group. After seeding the VECs, both the VSMCs in the matrix and the VECs in the lumen steadily proliferated with time. After differentiation culture, the markers of α-SMA and CD31 were stained and significantly observed in vessel matrices and lumen, respectively, indicating angiogenesis in the vessel. These results were also confirmed by the quantitative gene (α-SMA, vWf, and CD31) analysis which suggested angiogenesis expression in the bioprinted blood vessels. The novel bioprinted blood vessel with biomimetic endothelial and smooth muscle cell layers could be a potential candidate for future small-diameter blood vessel replacements.

■ ASSOCIATED CONTENT

Supporting Information

The Supporting Information is available free of charge at https://pubs.acs.org/doi/10.1021/acsami.0c14871.

Stress–strain curve and Young's modulus of biomimetic blood vessels (PDF)

■ AUTHOR INFORMATION

Corresponding Author

Lijie Grace Zhang – *Department of Mechanical and Aerospace Engineering, Department of Biomedical Engineering, Department of Electrical and Computer Engineering, and Department of Medicine, The George Washington University, Washington, District of Columbia 20052, United States;* orcid.org/0000-0003-3009-045X; Phone: 202-994-2479; Email: lgzhang@gwu.edu; Fax: 202-994-0238

Authors

Xuan Zhou – *Department of Mechanical and Aerospace Engineering, The George Washington University, Washington, District of Columbia 20052, United States*

Margaret Nowicki – *Department of Civil and Mechanical Engineering, The United States Military Academy, West Point, New York 10996, United States*

Hao Sun – *Department of Mechanical and Aerospace Engineering, The George Washington University, Washington, District of Columbia 20052, United States*

Sung Yun Hann – *Department of Mechanical and Aerospace Engineering, The George Washington University, Washington, District of Columbia 20052, United States*

Haitao Cui – *Department of Mechanical and Aerospace Engineering, The George Washington University, Washington, District of Columbia 20052, United States*

Timothy Esworthy – *Department of Mechanical and Aerospace Engineering, The George Washington University, Washington, District of Columbia 20052, United States*

James D. Lee – *Department of Mechanical and Aerospace Engineering, The George Washington University, Washington, District of Columbia 20052, United States*

Michael Plesniak – *Department of Mechanical and Aerospace Engineering, The George Washington University, Washington, District of Columbia 20052, United States*

Complete contact information is available at: https://pubs.acs.org/10.1021/acsami.0c14871

Notes

The authors declare no competing financial interest.

■ ACKNOWLEDGMENTS

The authors would like to thank the financial support from NSF BMMB program grant # 1854415, NIH Director's New Innovator Award 1DP2EB020549-01, and the George Washington University Center for Microscopy and Image Analysis for imaging support.

■ REFERENCES

(1) Novosel, E. C.; Kleinhans, C.; Kluger, P. J. Vascularization Is the Key Challenge in Tissue Engineering. *Adv. Drug Deliv. Rev.* **2011**, *63*, 300–311.

(2) Seifu, D. G.; Purnama, A.; Mequanint, K.; Mantovani, D. Small-Diameter Vascular Tissue Engineering. *Nat. Rev. Cardiol.* **2013**, *10*, 410–421.

(3) Cui, H.; Zhu, W.; Huang, Y.; Liu, C.; Yu, Z.-X.; Nowicki, M.; Miao, S.; Cheng, Y.; Zhou, X.; Lee, S.-J.; Zhou, Y.; Wang, S.; Mohiuddin, M.; Horvath, K.; Zhang, L. G. In Vitro and in Vivo Evaluation of 3d Bioprinted Small-Diameter Vasculature with Smooth Muscle and Endothelium. *Biofabrication* **2019**, *12*, 015004.

(4) Pashneh-Tala, S.; MacNeil, S.; Claeyssens, F. The Tissue-Engineered Vascular Graft-Past, Present, and Future. *Tissue Eng., Part B* **2016**, *22*, 68−100.
(5) Carrabba, M.; Madeddu, P. Current Strategies for the Manufacture of Small Size Tissue Engineering Vascular Grafts. *Front. Bioeng. Biotechnol.* **2018**, *6*, 41.
(6) Dahl, S. L. M.; Kypson, A. P.; Lawson, J. H.; Blum, J. L.; Strader, J. T.; Li, Y.; Manson, R. J.; Tente, W. E.; DiBernardo, L.; Hensley, M. T.; Carter, R.; Williams, T. P.; Prichard, H. L.; Dey, M. S.; Begelman, K. G.; Niklason, L. E. Readily Available Tissue-Engineered Vascular Grafts. *Sci. Transl. Med.* **2011**, *3*, 68ra9.
(7) Cho, S.-W.; Lim, S. H.; Kim, I.-K.; Hong, Y. S.; Kim, S.-S.; Yoo, K. J.; Park, H.-Y.; Jang, Y.; Chang, B. C.; Choi, C. Y.; Hwang, K.-C.; Kim, B.-S. Small-Diameter Blood Vessels Engineered with Bone Marrow-Derived Cells. *Ann. Surg.* **2005**, *241*, 506−515.
(8) Vaz, C. M.; van Tuijl, S.; Bouten, C. V. C.; Baaijens, F. P. T. Design of Scaffolds for Blood Vessel Tissue Engineering Using a Multi-Layering Electrospinning Technique. *Acta Biomater.* **2005**, *1*, 575−582.
(9) Awad, N. K.; Niu, H.; Ali, U.; Morsi, Y. S.; Lin, T. Electrospun Fibrous Scaffolds for Small-Diameter Blood Vessels: A Review. *Membranes* **2018**, *8*, 15.
(10) Hasan, A.; Memic, A.; Annabi, N.; Hossain, M.; Paul, A.; Dokmeci, M. R.; Dehghani, F.; Khademhosseini, A. Electrospun Scaffolds for Tissue Engineering of Vascular Grafts. *Acta Biomater.* **2014**, *10*, 11−25.
(11) Weinberg, C.; Bell, E. A Blood Vessel Model Constructed from Collagen and Cultured Vascular Cells. *Science* **1986**, *231*, 397−400.
(12) Niklason, L. E.; Gao, J.; Abbott, W. M.; Hirschi, K. K.; Houser, S.; Marini, R.; Langer, R. Functional Arteries Grown in Vitro. *Science* **1999**, *284*, 489−493.
(13) Quint, C.; Kondo, Y.; Manson, R. J.; Lawson, J. H.; Dardik, A.; Niklason, L. E. Decellularized Tissue-Engineered Blood Vessel as an Arterial Conduit. *Proc. Natl. Acad. Sci. U.S.A.* **2011**, *108*, 9214−9219.
(14) Radke, D.; Jia, W.; Sharma, D.; Fena, K.; Wang, G.; Goldman, J.; Zhao, F. Tissue Engineering at the Blood-Contacting Surface: A Review of Challenges and Strategies in Vascular Graft Development. *Adv. Healthc. Mater.* **2018**, *7*, 1701461.
(15) Xu, C. Y.; Inai, R.; Kotaki, M.; Ramakrishna, S. Aligned Biodegradable Nanofibrous Structure: A Potential Scaffold for Blood Vessel Engineering. *Biomaterials* **2004**, *25*, 877−886.
(16) Coultas, L.; Chawengsaksophak, K.; Rossant, J. Endothelial Cells and Vegf in Vascular Development. *Nature* **2005**, *438*, 937−945.
(17) Boerckel, J. D.; Uhrig, B. A.; Willett, N. J.; Huebsch, N.; Guldberg, R. E. Mechanical Regulation of Vascular Growth and Tissue Regeneration in Vivo. *Proc. Natl. Acad. Sci. U.S.A.* **2011**, *108*, E674−E680.
(18) Lacolley, P.; Regnault, V.; Nicoletti, A.; Li, Z.; Michel, J.-B. The Vascular Smooth Muscle Cell in Arterial Pathology: A Cell That Can Take on Multiple Roles. *Cardiovasc. Res.* **2012**, *95*, 194−204.
(19) Zhou, X.; Castro, N. J.; Zhu, W.; Cui, H.; Aliabouzar, M.; Sarkar, K.; Zhang, L. G. Improved Human Bone Marrow Mesenchymal Stem Cell Osteogenesis in 3d Bioprinted Tissue Scaffolds with Low Intensity Pulsed Ultrasound Stimulation. *Sci. Rep.* **2016**, *6*, 32876.
(20) Zhou, X.; Zhu, W.; Nowicki, M.; Miao, S.; Cui, H.; Holmes, B.; Glazer, R. I.; Zhang, L. G. 3d Bioprinting a Cell-Laden Bone Matrix for Breast Cancer Metastasis Study. *ACS Appl. Mater. Interfaces* **2016**, *8*, 30017−30026.
(21) Cui, H.; Miao, S.; Esworthy, T.; Zhou, X.; Lee, S.-j.; Liu, C.; Yu, Z.-x.; Fisher, J. P.; Mohiuddin, M.; Zhang, L. G. 3d Bioprinting for Cardiovascular Regeneration and Pharmacology. *Adv. Drug Deliv. Rev.* **2018**, *132*, 252−269.
(22) Minto, J.; Zhou, X.; Osborn, J.; Zhang, L. G.; Sarkar, K.; Rao, R. D. Three-Dimensional Printing: A Catalyst for a Changing Orthopaedic Landscape. *JBJS Rev.* **2020**, *8*, e0076.
(23) Hann, S. Y.; Cui, H.; Esworthy, T.; Miao, S.; Zhou, X.; Lee, S.-j.; Fisher, J. P.; Zhang, L. G. Recent Advances in 3d Printing: Vascular Network for Tissue and Organ Regeneration. *Transl. Res.* **2019**, *211*, 46−63.
(24) Murphy, S. V.; Atala, A. 3d Bioprinting of Tissues and Organs. *Nat. Biotechnol.* **2014**, *32*, 773−785.
(25) Gao, G.; Cui, X. Three-Dimensional Bioprinting in Tissue Engineering and Regenerative Medicine. *Biotechnol. Lett.* **2016**, *38*, 203−211.
(26) Zhou, X.; Esworthy, T.; Lee, S.-J.; Miao, S.; Cui, H.; Plesiniak, M.; Fenniri, H.; Webster, T.; Rao, R. D.; Zhang, L. G. 3d Printed Scaffolds with Hierarchical Biomimetic Structure for Osteochondral Regeneration. *Nanomedicine* **2019**, *19*, 58−70.
(27) Kolesky, D. B.; Homan, K. A.; Skylar-Scott, M. A.; Lewis, J. A. Three-Dimensional Bioprinting of Thick Vascularized Tissues. *Proc. Natl. Acad. Sci. U.S.A.* **2016**, *113*, 3179−3184.
(28) Tang, J.; Bao, L.; Li, X.; Chen, L.; Hong, F. F. Potential of Pva-Doped Bacterial Nano-Cellulose Tubular Composites for Artificial Blood Vessels. *J. Mater. Chem. B* **2015**, *3*, 8537−8547.
(29) Zhou, X.; Nowicki, M.; Cui, H.; Zhu, W.; Fang, X.; Miao, S.; Lee, S.-J.; Keidar, M.; Zhang, L. G. 3d Bioprinted Graphene Oxide-Incorporated Matrix for Promoting Chondrogenic Differentiation of Human Bone Marrow Mesenchymal Stem Cells. *Carbon* **2017**, *116*, 615−624.
(30) Zhou, X.; Cui, H.; Nowicki, M.; Miao, S.; Lee, S.-J.; Masood, F.; Harris, B. T.; Zhang, L. G. Three-Dimensional-Bioprinted Dopamine-Based Matrix for Promoting Neural Regeneration. *ACS Appl. Mater. Interfaces* **2018**, *10*, 8993−9001.
(31) Colosi, C.; Shin, S. R.; Manoharan, V.; Massa, S.; Costantini, M.; Barbetta, A.; Dokmeci, M. R.; Dentini, M.; Khademhosseini, A. Microfluidic Bioprinting of Heterogeneous 3d Tissue Constructs Using Low-Viscosity Bioink. *Adv. Mater.* **2016**, *28*, 677−684.
(32) Lee, K. Y.; Mooney, D. J. Alginate: Properties and Biomedical Applications. *Prog. Polym. Sci.* **2012**, *37*, 106−126.
(33) Issa, B.; Moore, R. J.; Bowtell, R. W.; Baker, P. N.; Johnson, I. R.; Worthington, B. S.; Gowland, P. A. Quantification of Blood Velocity and Flow Rates in the Uterine Vessels Using Echo Planar Imaging at 0.5 Tesla. *J. Magn. Reson. Imag.* **2010**, *31*, 921−927.
(34) Zhou, X.; Cheng, X. J.; Liu, W. F.; Li, J. J.; Ren, L. H.; Dang, Q. F.; Feng, C.; Chen, X. G. Optimization and Characteristics of Preparing Chitosan Microspheres Using Response Surface Methodology. *J. Appl. Polym. Sci.* **2013**, *127*, 4433−4439.
(35) Wang, Q. Q.; Kong, M.; An, Y.; Liu, Y.; Li, J. J.; Zhou, X.; Feng, C.; Li, J.; Jiang, S. Y.; Cheng, X. J.; Chen, X. G. Hydroxybutyl Chitosan Thermo-Sensitive Hydrogel: A Potential Drug Delivery System. *J. Mater. Sci.* **2013**, *48*, 5614−5623.
(36) Zhu, B.; Yin, H. Alginate Lyase: Review of Major Sources and Classification, Properties, Structure-Function Analysis and Applications. *Bioengineered* **2015**, *6*, 125−131.
(37) Ebrahimi, A. P. Mechanical Properties of Normal and Diseased Cerebrovascular System. *J. Vasc. Interv. Neurol.* **2009**, *2*, 155−162.
(38) Gauvin, R.; Guillemette, M.; Galbraith, T.; Bourget, J. M.; Larouche, D.; Marcoux, H.; Aube, D.; Hayward, C.; Auger, F. A.; Germain, L. Mechanical Properties of Tissue-Engineered Vascular Constructs Produced Using Arterial or Venous Cells. *Tissue Eng., Part A* **2011**, *17*, 2049−2059.
(39) Çinar, Y.; Şenyol, A. M.; Duman, K. Blood Viscosity and Blood Pressure: Role of Temperature and Hyperglycemia. *Am. J. Hypertens.* **2001**, *14*, 433−438.
(40) Hinz, B.; Celetta, G.; Tomasek, J. J.; Gabbiani, G.; Chaponnier, C. Alpha-Smooth Muscle Actin Expression Upregulates Fibroblast Contractile Activity. *Mol. Biol. Cell* **2001**, *12*, 2730−2741.
(41) Pusztaszeri, M. P.; Seelentag, W.; Bosman, F. T. Immunohistochemical Expression of Endothelial Markers Cd31, Cd34, Von Willebrand Factor, and Fli-1 in Normal Human Tissues. *J. Histochem. Cytochem.* **2006**, *54*, 385−395.
(42) Sadler, J. E. Biochemistry and Genetics of Von Willebrand Factor. *Annu. Rev. Biochem.* **1998**, *67*, 395−424.
(43) Starke, R. D.; Ferraro, F.; Paschalaki, K. E.; Dryden, N. H.; McKinnon, T. A. J.; Sutton, R. E.; Payne, E. M.; Haskard, D. O.; Hughes, A. D.; Cutler, D. F.; Laffan, M. A.; Randi, A. M. Endothelial Von Willebrand Factor Regulates Angiogenesis. *Blood* **2011**, *117*, 1071−1080.

https://dx.doi.org/10.1021/acsami.0c14871
ACS Appl. Mater. Interfaces 2020, 12, 45904−45915